Applied Surface Science 315 (2014) 481–489

Contents lists available at ScienceDirect

Applied Surface Science

journal homepage: www.elsevier.com/locate/apsusc

Plasma electrolytic oxide coatings on valve metals and their activity in CO oxidation

I.V. Lukiyanchuk[a,*], V.S. Rudnev[a,b], L.M. Tyrina[a], I.V. Chernykh[a]

[a] *Institute of Chemistry, Far-Eastern Branch of Russian Academy of Sciences, Prosp. 100-letiya Vladivostoka 159, 690022, Russia*
[b] *Far Eastern Federal University, Sukhanova 8, Vladivostok 690950, Russia*

ARTICLE INFO

Article history:
Received 28 December 2013
Received in revised form 6 March 2014
Accepted 7 March 2014
Available online 15 March 2014

Keywords:
Plasma electrolytic oxidation
Impregnation
Coatings
Transition metal oxides
Platinum
CO oxidation

ABSTRACT

Two approaches have been examined for obtaining titanium- or aluminum-supported catalysts with transition and noble metals using the plasma electrolytic oxidation (PEO) technique. Elemental compositions, distribution of active elements and catalytic activity in CO oxidation have been compared for composites formed by one-stage PEO technique and those obtained as a result of modification of PEO coatings by impregnation.

1. Introduction

Plasma electrolytic oxidation consists in anode or anode–cathode processing valve metals under spark or arc electric discharges. Alternative terms for PEO can include: anode spark electrolysis, anodic oxidation under spark discharge, microplasma anodizing, micro arc oxidation, anodic discharge anodizing, and anodic spark deposition [1–4]. Electrical breakdowns of an anode film produce high temperatures and pressures in discharge channels and around them, which results in the thermolysis of electrolyte components and their incorporating into growing coating structures. As a result, obtaining coatings of various compositions is made possible. Moreover, this is the way for preparing both secondary substrates [5–7] and catalytic oxide layers [8–12] on metal substrates, which are promising as heterogeneous catalysts [7–10,13,14], photo-catalysts [15–22], and active [11,23,24] and indicator electrodes [25].

The paper considers two possibilities of PEO application for obtaining catalytically active oxide layers on aluminum and titanium. The first one is one-stage PEO technique, in which precursors of catalytically active compounds are directly included in the forming electrolyte. The method ensures the formation of oxide layers with controlled porosity and their conversion into target catalytically active coatings in a continuous one-pot process by choosing appropriate electrolyte compositions [8]. This approach was used to obtain the coatings demonstrating catalytic activity in deep oxidation of propane–butane mixture [10] and catalytic cracking reactions [11], as well as in oxydehydrogenation of cyclohexane to cyclohexene [8,9] and phenol oxidation [26]. The advantages of composites obtained consist in the combination of high thermal stability due to the substrate metal with high corrosion and wear resistance of the coating. The disadvantages include a low surface area (0.2–0.7 m^2/g [8]) and the necessity to work at high temperatures limiting the working temperature range by the melting point of the substrate metal.

The second approach is related to modification of PEO coatings (secondary substrates) using other methods such as impregnation in precursor solutions [5,6], extraction pyrolysis [7,27], and template synthesis [28]. The combination of PEO technique and impregnation has been examined in more detail [5,6,29,30]. An additional application of the impregnation technique followed by annealing enables one to increase the surface area 5–10-fold [31] and higher, for example, thanks to the whiskers growth on the modified surface [6,32]. The composites ‘modified PEO coating/valve metal’ can find application in afterburning of exhaust gases of vehicles and industrial plants [5], combustion of diesel soot [7], and

---

[*] Corresponding author. Tel.: +7 423 2215265; fax: +7 423 2312590.
E-mail address: lukiyanchuk@ich.dvo.ru (I.V. Lukiyanchuk).

http://dx.doi.org/10.1016/j.apsusc.2014.03.040
0169-4332/

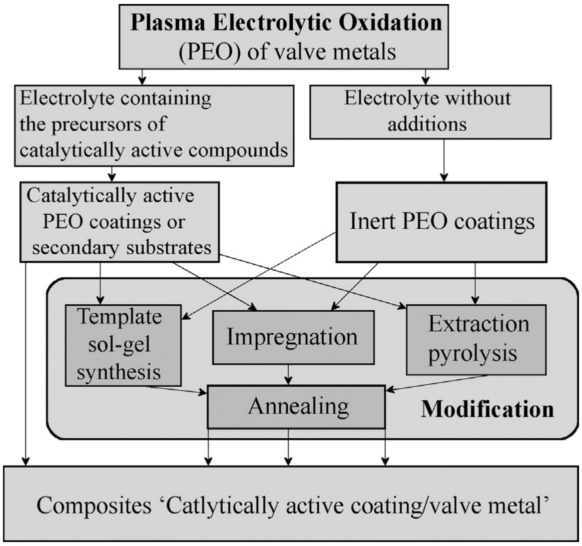

Fig. 1. Diagram of using PEO technique for obtaining catalytically active structures on valve metals.

biomass gasification [6]. Initial PEO layers (prior to modification) can be inert or have an intrinsic catalytic activity. In the latter case, the best result is achieved.

Some possibilities of PEO technique for preparation of catalytically active composites based on valve metals are summarized in Fig. 1.

The objective of the present work consists in comparing the composition, morphology, and catalytic activity in CO oxidation of the coatings with transition (Mn, Fe, Co, Ni, Cu) and noble metals (Pt) obtained on aluminum and titanium by one-stage plasma electrolytic oxidation with those of the coatings obtained by combination of PEO with the impregnation technique.

2. Experimental

2.1. Materials

The PEO layers were formed on aluminum alloys AMg5 (4.8–5.8% Mg, 0.02–0.01% Ti, and the balance Al) and AMtsM (Al + 1.6% Mn) and titanium VT1-0 (Ti content > 99.6%). Two types of samples were used: flat samples of 20 × 20 × 1 mm were used to determine the elemental and phase composition of the surface and to measure the thickness of coatings, whereas catalytic tests were performed with Al and Ti wire (1.67 and 1.2 mm in diameter, respectively) samples with a working surface area 20 cm^2. To standardize pre-coating sample surfaces, they were chemically polished to high luster (surface finish class 8–9) in a mixture of concentrated acids. A mixture of H_3PO_4:H_2SO_4:HNO_3 = 4:2:1 (by volume) at 110–120 °C and a mixture of HF:HNO_3 = 1:3 (by volume) at 70 °C were used for treating aluminum and titanium, respectively. Then the samples were washed with distilled water and dried by air at 70 °C.

2.2. PEO treatment

The PEO treatment of titanium and aluminum samples was carried out in a thermal glass of a volume of 1 L. The computer-controlled thyristor unit TER-100/460H (Russia) with unipolar pulse current was used as a power source. The sample under treatment was connected with a positive pole of the power supply while a spiral-shaped stainless steel coil cooled with tap water served as a cathode. The electrolyte in a glass was agitated using a magnetic mixer. The electrolyte temperature was maintained below 35 °C during the process. After the PEO treatment, the samples were rinsed by the distilled water and air-dried at room temperature.

2.3. Coating formation

Two methods were used for preparing both coatings with transition metal compounds and Pt-containing ones: one-stage plasma electrolytic oxidation (method I) and combination of this technique with impregnation followed by air annealing (method II).

2.3.1. M- and Cu-containing coatings (where M = Mn, Fe, Co, Ni)

Method I: In this case the M- and Cu-containing coatings (where M = Mn, Fe, Co, Ni) on the AMg5 aluminum alloy were formed by one-stage PEO technique using corresponding electrolytes based on an aqueous phosphate–borate–tungstate solution (hereinafter referred to as PBW [33]). This solution consists of 0.066 mol/L Na_3PO_4, 0.034 mol/L $Na_2B_4O_7$, and 0.006 mol/L Na_2WO_4. It enables one to obtain corrosion-resistant layers including γ-Al_2O_3. Furthermore, alkaline electrolytes (PBW among them) produce corresponding hydroxide precipitates upon addition of transition metal salts, which is important for formation of multiphase oxide structures by PEO on the surface of the metals under treatment [34]. As was shown earlier [35], PEO-coatings simultaneously containing two transition metals (nickel and copper) were more active and stable than the coatings with only one transition metal in their composition. Therefore, we added soluble salts of copper and a salt of transition metal M (where M is Mn, Fe, Co, Ni) into the PBW-electrolyte. The electrolytes referred to as PBWMnCu, PBWFeCu, PBWCoCu, and PBWNiCu contained 0.025 mol/L of $Cu(CH_3COO)_2$ and 0.08 mol/L of another transition metal (0.08 mol/L $Mn(CH_3COO)_2$ or $Co(CH_3COO)_2$ or $Ni(CH_3COO)_2$ or 0.04 mol/L $Fe_2(C_2O_4)_3$). Oxide layers were formed at an effective current density of 10 or 20 A/dm^2 for 5 or 10 min. Details are described in [36] and given in Table 1.

Method II ("PEO + impregnation"): Oxide layers or secondary carriers were preliminary formed on AMg5 aluminum alloy or on titanium by the PEO technique at an effective current density of 10 A/dm^2 for 10 min in the silicate alkaline electrolyte 0.05 mol/L Na_2SiO_3 + 0.05 mol/L NaOH (Table 1). For deposition of transition metal binary oxides, the PEO-coated samples were exposed to an aqueous solution for 1 h containing 1.0 mol/L $Cu(NO_3)_2$ and 1.0 mol/L of one of the nitrates of another transition metal (Mn(II), Fe(III), Co(II) or Ni(II)), with consecutive drying and air annealing in a muffle furnace at 500 °C for 4 h. Details are described in [37].

Table 1
One-stage formation on aluminum alloy and titanium of PEO coatings containing transition metal compounds.

PEO conditions					Coating thickness, µm
Substrate metal	Electrolyte	*i*, A/cm^2	*t*, min	U_f, V	
Al	PBWMnCu	0.2	5	371	21.7 ± 0.8
Al	PBWFeCu	0.1	10	70	33.3 ± 0.8
Al	PBWCoCu	0.1	10	271	11.5 ± 0.7
Al	PBWNiCu	0.1	10	351	14.0 ± 1.0
Al	0.05 mol/L Na_2SiO_3 + 0.05 mol/L NaOH	0.1	10	360	9.0 ± 0.9
Ti	0.05 mol/L Na_2SiO_3 + 0.05 mol/L NaOH	0.1	10	250	13.0 ± 1.0

Table 2
Formation conditions of Pt-containing coatings, their phase compositions and active element contents.

Substrate metal	Method	PEO conditions		Impregnation details		Phase composition	Concentration of active elements, at.%		Symbolic representation (system)	Ref.
		Electrolyte, mol/L	Regime	Concentration of H_2PtCl_6, mol/L	*N*		XSA	XPS		
Al	I	0.049 $Na_6P_6O_{18}$ + 0.0029 H_2PtCl_6	AC 50 Hz, $i = 0.2$ A/cm^2 $t = 10$ min			γ-Al_2O_3	0.08 Pt	1.7/2.7 Pt	0.08 Pt + γ-Al_2O_3/Al (Pt-Al)	[38,39]
Ti	I	0.049 $Na_6P_6O_{18}$ + 0.0029H_2PtCl_6	DC $i = 0.05$ A/cm^2 $t = 6$ min			TiO_2 (a), Pt	0.95 Pt	0.7/1.5 Pt	0.95 Pt + TiO_2/Ti (Pt-Ti)	[39]
Ti	I	0.0245 $Zr(SO_4)_2$ + 0.0245 $Ce_2(SO_4)_3$ + 0.0019 H_2PtCl_6	DC $i = 0.2$ A/cm^2 $t = 10$ min			TiO_2 (a, r)	0 Pt, 1.7 Ce, 1.4 Zr	0.1/0.1 Pt, 0.7/3.7 Ce, 2.1/4.4 Zr	Pt + Ce_2O_3 + ZrO_2 + TiO_2/Ti (Pt–Ce–Zr–Ti)	[39]
Ti	I	0.0245 $Zr(SO_4)_2$ + 0.0245 $Ce_2(SO_4)_3$ + 0.0019 H_2PtCl_6	AC $i_a = -i_c = 0.2$ A/cm^2 $\tau_a = \tau_c = 0.02$ s			TiO_2 (a, r), Pt	0.85 Pt, 1.1 Ce, 2.2 Zr	0.2/0.5 Pt, 0.8/2.4 Ce, 3.8/6.7 Zr	0.85 Pt + Ce_2O_3 + ZrO_2 + TiO_2/Ti (Pt–Ce–Zr–Ti)	[39]
Al	II	PBW	DC $i = 0.1$ A/cm^2 $t = 10$ min	0.038	1	γ-Al_2O_3, Pt-traces	0.1 Pt		0.1 Pt/γ-Al_2O_3/Al (Pt-Al)	[40]
Al	II	PBW	DC $i = 0.1$ A/cm^2 $t = 10$ min	0.038	2	γ-Al_2O_3, Pt	0.2 Pt	0.5/1.0 Pt	0.2 Pt/γ-Al_2O_3/Al (Pt–Al)	[40]
Al	II	PBWNiCu	DC $i = 0.1$ A/cm^2 $t = 10$ min	0.038	1	γ-Al_2O_3	0.1 Pt, 1.4Ni	1.0/1.5 Pt 1.4/2.2 Ni 0.9/0.7 Cu	0.1 Pt/NiO + CuO + γ-Al_2O_3/Al (Pt-Ni-Cu-Al)	[40]
Ti	II	0.0245 $Zr(SO_4)_2$ + 0.0245 $Ce_2(SO_4)_3$	DC $i = 0.05$ A/cm^2 $t = 7$ min	0.0029	1	TiO_2 (a, r)	0 Pt, 1.5 Ce, 3.6 Zr	0.4/0.4 Pt 1.2/3.0 Ce 12.8/15.3 Zr	Pt/Ce_2O_3 + ZrO_2 + TiO_2/Ti (Pt–Ce–Zr–Ti)	[29]
Ti	II	0.049 $Zr(SO_4)_2$	DC $i = 0.05$ A/cm^2 $t = 7$ min	0.0029	1	ZrO_2 (c), $ZrTiO_4$, TiO_2 (a, r)	0 Pt, 8.3Zr		Pt/ZrO_2,TiO_2/Ti (Pt–Zr–Ti)	[29]

Notes: a – anatase, r – rutile, c – cubic, *N* – number of impregnation cycles.

2.3.2. Pt-containing coatings

Method I: Two electrolyte solutions were chosen to obtain Pt-containing coatings on titanium and aluminum by one-stage PEO technique. The first contained sodium hexametaphosphate and chloroplatinic acid: it was used for oxidation of both aluminum and titanium. The second consisted of zirconium and cerium sulfates and chloroplatinic acid. It was used only for titanium because sulfates have an etching effect on aluminum and its alloys. The conditions of PEO treatment and features of electrolyte preparations are described in [38,39] and given in Table 2.

Method II ("PEO + impregnation"): PEO layers on aluminum alloy were formed in PBW- and PBWNiCu-electrolytes and those on titanium were obtained in $Zr(SO_4)_2 + Ce_2(SO_4)_3$ electyrolyte. In order to incorporate platinum into oxide layers the coated samples were immersed into aqueous solution of 2.9×10^{-3}–3.8×10^{-2} mol/L H_2PtCl_6 for 3–15 min. Then coatings were air-dried at 120 °C and annealed during 2 h at 450–500 °C in muffle furnace. In some experiments impregnation was performed twice to increase the introduced platinum amount in the coating. Details are represented in papers [29,40] and Table 2.

2.4. Composite examination

The thickness of coatings was measured using an eddy-current thickness gage VT-201 (Russia). The surface morphology and element composition data (X-ray spectrum analysis, XSA, average readings from areas $50 \times 50\ \mu m^2$, 2–5 μm deep) were obtained by an electron probe micro-analyzer JXA 8100 (Japan) with an INCA energy spectrum analyzer (United Kingdom). To prevent surface charging, a thin layer of chromium or carbon was deposited on the samples prior to measuring. The X-ray diffraction (XRD) patterns were studied with a D8 Advance X-ray diffractometer (Germany) using CuK_α radiation. The relevant analysis was carried out using the EVA retrieval program and the PDF-2 database.

X-ray photoelectron spectroscopy (XPS) was also used to describe the surfaces: the Specs ultra high-vacuum system with a 150-mm electrostatic hemispherical analyzer. Ionization was implemented using the MgKα radiation. The spectra were calibrated on the C1s line of hydrocarbons, whose energy was assumed to be 285.0 eV, whereas the surface was etched by argon ions (with 5 keV energy) bombarding.

2.5. Catalytic testing

The catalytic tests in CO oxidation reaction were performed using a *BI-CATflow* 4.2(A) multipurpose flow system (Boreskov Institute of Catalysis, Siberian Branch, Russian Academy of Sciences). Finely cut wire samples with coatings were placed in the active zone of a quartz tube reactor of a size of 0.9 cm (diameter) × 3 cm (height). The geometric surface area of the catalyst outer layer on the aluminum or titanium alloy was 20 cm^2. The preliminary tests showed that CO conversion on the metal supports without PEO coatings was not higher than 10% in the test temperature range (from 20 to 500 °C). The initial reaction mixture contained 5% CO and 95% air, with the gas flow rate equal to 50 ml/min. The outlet concentrations of CO and CO_2 were determined using a PEM-2 IR gas analyzer. In this case, the activity of the samples was judged by the temperature dependence of CO conversion and the temperature of half-conversion T_{50} (that is the temperature when conversion CO achieved 50%).

Some samples with coatings were additionally tested using BI-CATr-EXP flow circulating system (Boreskov Institute of Catalysis, Siberian Branch, RAS), which allows evaluating the activation energy and the reaction rate.

3. Results and discussion

3.1. M + Cu-containing coatings

Table 3 provides the *elemental and phase composition* of the coatings formed by methods I and II.

According to XRD, crystalline transition metal oxides are found only in the composition of Co-, Cu-containing and Mn-, Cu-containing coatings, obtained by one-stage PEO technique (method I). In the case of Fe-, Cu-containing and Ni-, Cu-containing coatings, transition metals seem to be in the amorphous phase compositions.

At the same time, crystalline transition metal oxides are found in the composition of all coatings obtained by the combination of PEO and impregnation (method II). Copper oxide was detected in all cases except the Ni-, Cu-containing structures on titanium. Manganese and iron oxides were not found in the composition of Mn-, Cu- and Fe-, Cu-containing coatings on aluminum alloy. Taking into account rather high concentrations of these metals in the coatings, one can assume that their compounds are present in amorphous or fine-crystalline forms.

As regards the decrease of total concentration of transition elements (M + Cu) determined by the X-ray spectrum analysis (XSA), Table 3, the composites can be ranged as follows:

AMg5-I : Fe–Cu > Mn–Cu > Co–Cu > Ni–Cu;

AMg5-II : Fe–Cu > Co–Cu > Ni–Cu > Mn–Cu;

VT1-0-II : Fe–Cu > Mn–Cu > Co–Cu > Ni–Cu.

Table 3
Impact of preparation technique and substrate metal on elemental and phase composition of M + Cu-containing coatings.

Alloy	Method	PEO-layer/Al(Ti)	Phase composition				Elemental composition			
			Mn–Cu	Fe–Cu	Co–Cu	Ni-–Cu	Mn–Cu	Fe–Cu	Co–Cu	Ni–Cu
AMg5	I	PBWMCu/Al	$MnO_2 + MnO$	Amorphous	γ-Al_2O_3 + $CoAl_2O_4$ + Co_3O_4 + $CuAl_2O_4$ + ?Co	γ-Al_2O_3	11.0 Mn, 0.8 Cu, 2.9P, 0.7 W, 1.3 Mg, 25.0 Al, 58.3 O,	21.0Fe, 2.3Cu, 9.3P, 1.2 W 2.2 Na, 5.8Al, 58.2 O	5.7Co, 0.5 Cu, 1.0P, 0.4 W, 1.4 Mg, 35.8Al, 55.2 O	4.8Ni, 0.6 Cu, 1.0P, 0.1 W, 1.8 Mg, 36.8 Al, 54.9 O
AMg5	II	$\underline{M_xO_y} + \underline{CuO}$ $\underline{SiO_2} + \underline{Al_2O_3}$ Al	Cu_4O_3 γ-Al_2O_3	CuO, γ-Al_2O_3	Co_3O_4, CuO, γ-Al_2O_3	CuO, NiO, γ-Al_2O_3	3.4 Mn, 3.2Cu, 7.8Si, 17.3 C, 15.9Al, 52.2 O	12.1 Fe, 14.7Cu, 9.6C, 0.7 Mg, 7.3Al, 54.6 O	6.8 Co, 6.9Cu, 8.1Si, 11.0 C, 1.2 Mg, 14.5Al, 51.5 O	5.5 Ni, 5.0Cu, 8.9Si, 11.2 C, 1.3 Mg, 16.5Al, 51.5 O
VT1-0	II	$\underline{M_xO_y} = + \underline{CuO}$ $\underline{SiO_2} + \underline{TiO_2}$ Ti	Mn_2O_3, CuO (tenorite), $Cu_{1.5}Mn_{1.5}O_4$, TiO_2 (rutile, anatase)	CuO, γ-Fe_2O_3, TiO_2 (rutile, anatase)	CuO, Co_3O_4, TiO_2 (rutile, anatase)	NiO,TiO_2 (anatase)	4.1 Mn, 4.0Cu, 9.3Si, 6.9 C, 10.2 Ti, 65.5 O	9.1 Fe, 10.6Cu, 5.8Si, 13.6 C, 6.1 Ti, 54.8O	3.8 Co, 3.3 Cu, 8.6Si, 20.0 C, 8.4 Ti, 55.7O	2.0 Cu, 3.6 Ni, 8.2Si, 15.5 C, 11.8 Ti, 58.9O

In all cases, the highest total concentration of M + Cu is related to Fe-, Cu-containing composites, while the lowest total concentration characterizes those containing Ni, Cu and Mn, Cu.

Fig. 2 gives the composite surface morphologies. In case of coatings formed by one-stage PEO technique, their morphology depends on the forming electrolyte. For example, grain scattering occurs on the surface of coatings formed in the PBWNiCu electrolyte, while caverns (pores closed by lids) are typical for the coatings obtained in PBWMnCu. The surface of a layer formed in the PBWCoCu electrolyte has a finely porous structure, whereas that obtained in the PBWFe electrolyte contains a coarse relief fragments with fine pores.

Since all the impregnated composites formed by the method II usually duplicate the relief of the initial PEO-layer, their morphologies are similar.

One should mention the differences in element distributions on the surface of coatings obtained by the methods I and II. In the first case, transition metals are mainly concentrated in pores and microgranules on the surface of the PEO coatings [41–43]. In the latter case, the shell catalysts are formed from the transition metal oxides [37].

The transition metal distribution on the surface of impregnated coatings varies from one point to another as well. Table 4 shows the elemental composition of the individual morphological structures on the surface of Co-, Cu-containing coatings II shown by the numbers in Fig. 3. The smooth spots incorporate cobalt and copper in proportion to their concentration in the impregnating solution while the granules contain three times more copper than cobalt.

The catalytic activity of the compositions in CO oxidation was estimated by the conversion of temperature dependences and by the temperature of half-conversion T_{50}, Fig. 4. The compositions formed by the method II are obviously more active than those obtained by the method I. In the latter case, the half-conversion temperature is more than 100 °C higher than T_{50} for the impregnated compositions. Based on their decreasing catalytic activity (Fig. 4), the formed compositions 'M + Cu-containing coating/valve metal' were ranged as:

$$\text{AMg5-I}: \quad \text{Cu–Ni} > \text{Cu–Co} > \text{Cu–Fe} > \text{Cu–Mn};$$

$$\text{AMg5-II}: \quad \text{Co–Cu} > \text{Mn–Cu} \approx \text{Ni–Cu} > \text{Fe–Cu};$$

$$\text{VT1-0-II}: \quad \text{Co–Cu} > \text{Mn–Cu} > \text{Ni–Cu} > \text{Fe–Cu}.$$

It is evident that these rows of catalytic activity are not associated with total concentrations of active elements in the coating compositions. The difference between the activities rows can be explained by the presence of different compounds in coatings obtained by the methods I and II. On the surface of silicate PEO coatings (method II), the "crust" from transition metal oxides is formed as a result of thermal decomposition of nitrates. This crust fills roughnesses of PEO coating surfaces (Fig. 2). The row of catalytic activity drop for coatings II on titanium coincides with that for individual oxides of these transition metals in deep oxidation of carbon monoxide, which is related to the bonding energy of the surface oxygen (according to Boreskov data [44,45]). In this case, the silicate PEO coating behaves as an inert secondary substrate. Small variations in T_{50} for impregnated coatings II on aluminum alloy (Fig. 4b) can be related to the effect of γ-Al_2O_3, which is widely used as a substrate in heterogeneous catalysis.

PEO coatings formed in electrolytes of the PBWMCu-series contain not only transition metals, but also other components of electrolytes – P, B, and W. One should mention that the copper concentration in these coatings is far less than that in impregnated ones (Table 3). Moreover, the transition metals in the composition of such coatings can be concentrated in different morphological structures: nickel compounds form micrograins on the coatings surface, cobalt is concentrated in pores, while manganese is incorporated into molten surface structures. These facts may influence the catalytic activity of the formed structures.

3.2. *Pt-containing coatings*

Table 2 represents the phase composition as well as the platinum content in the coatings obtained by the methods I and II.

When the coatings are obtained by one-stage PEO technique, the concentration of H_2PtCl_6 in the forming electrolyte should be limited due to the etching action of chloride ions on the surface of metal under treatment during PEO process. The platinum content in the coatings formed by the method I depends on the forming electrolyte, current mode, and metal under treatment. For example, no platinum was found in coatings produced on titanium under anodic polarization in an electrolyte with zirconium and cerium salts, whereas in coatings obtained under anodic-cathodic polarization, its content approaches 1 at.%. Possibly, the processes of platinum deposition onto the electrode during cathodic pulses are important. The platinum concentration in coatings formed on titanium in phosphate electrolyte is 10 times higher than that in similar coatings on aluminum. According to XPS [38], platinum is concentrated on the surface and in subsurface layers on aluminum in the form of Pt^0. Platinum oxidation numbers on the surface and in subsurface layers of coatings on titanium are Pt^{2+} and Pt^{2+}, Pt^0, respectively.

Application of the method II enables one to increase the Pt content in the coatings on aluminum, first of all, because of the possibility to increase the concentration of H_2PtCl_6 in the impregnation solution and the number of operations. Impregnation results in the platinum concentration increase in surface layers of the coatings on titanium compared to those formed by the method I in sulfate ($Ce_2(SO_4)_3 + Zr(SO_4)_2$) electrolytes using the DC current mode.

Fig. 5 shows SEM images of Pt-containing coatings formed by methods I and II. The areas where platinum (heavy element) are located appear as white spots on the micrographs in a phase contrast regime. As can be seen from the comparison of Fig. 5a and b, platinum is differently distributed in surface components. The coatings obtained by the method I (Fig. 5a) contain arrays of disperse platinum-enriched particles of a size of ~1 μm, whereas platinum is concentrated around the pores of the coatings obtained by method II (Fig. 5b). In the former case the Pt concentration is 1.4 at.%, while in the latter case it reaches 6–51 at.% in some areas.

The mechanism of formation of amorphous or crystalline disperse particles on the surface of PEO coatings is discussed in [38,46]. It is related to the formation of disperse particles in local supersaturated solution regions near the anode–electrolyte interface under electrical discharge conditions. Colloidal particles of oxidized metal could serve as nucleation centers. Such particles are formed as a consequence of the emission of metal ions from the substrate to the solution by electrical discharges and the presence of hydroxyl groups at the anode. The forming disperse particles (microgranules) are driven by electrophoresis to the surface of the anodic oxide, where they are concentrated at defect sites, i.e., in zones with the highest electric field intensity.

Fig. 6 shows the change in the temperatures of half-conversion of CO T_{50} depending on the method of preparing the composites, electrolyte composition, and number of impregnation operations.

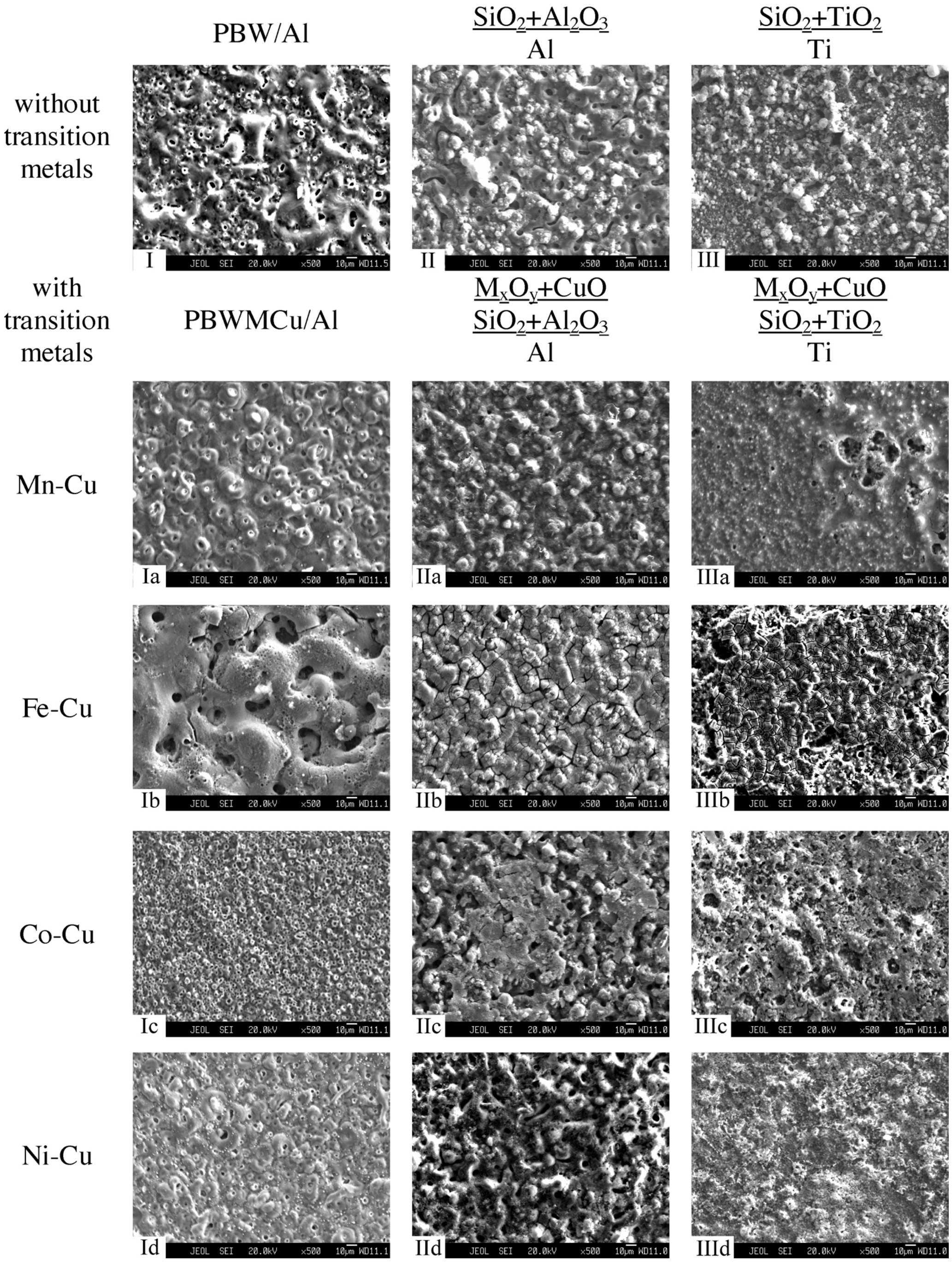

Fig. 2. SEM-images of initial coatings formed in electrolytes without transition metal compounds (I, II, III) and those of M-, Cu-containing coatings formed by methods I (Ia–Id) and II (IIa–IId and IIIa–IIId).

Table 4
Elemental composition of different structures on the surface of Co-, Cu-containing coating on titanium formed by method II.

Element	*C*, at.%				
	Fig. 3a			Fig. 3b	
	Surface (1)	Smooth spot (2)	Granule (3)	Smooth spot (2)	Granule (1)
C	17.07	14.09	15.23	12.43	14.71
O	44.01	47.66	48.72	48.86	49.89
Si	5.07	1.93	4.27	6.78	3.90
Ti	4.38	4.41	1.09	1.88	1.26
Co	13.38	16.59	7.17	15.68	7.20
Cu	16.08	15.31	23.51	14.37	23.03
Total	100	100	100	100	100

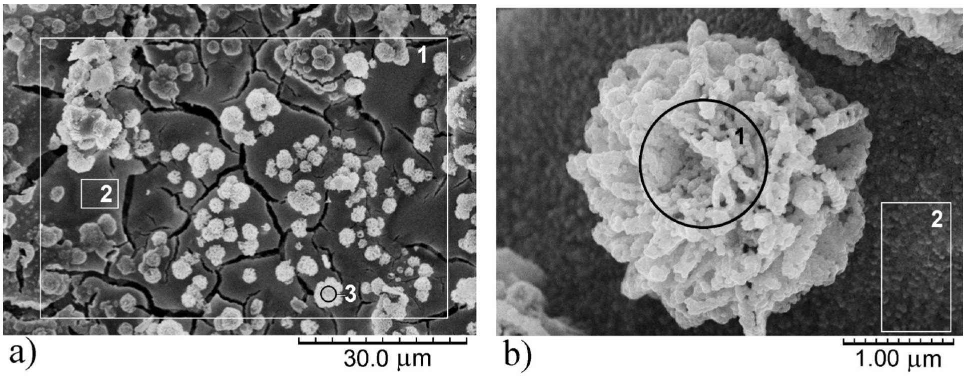

Fig. 3. SEM images of Co-, Cu-containing coatings on titanium formed by the combination of PEO and impregnation technique (method II). Numbers indicate the areas analyzed.

The coatings on aluminum and titanium obtained by one-stage PEO technique in phosphate electrolyte have similar activities in CO oxidation despite lower concentration of platinum in the coatings on aluminum.

For Pt–Ce–Zr–Ti systems, using the AC current mode results in more active coatings than in case of impregnation. However, when PEO treatment is performed in zirconium sulfate solution, more active coatings are obtained upon impregnation.

The following factors contributed to obtaining more catalytically active Pt–Al systems: the use of higher concentration of H_2PtCl_6, increasing multiplicity of impregnation, replacement of the PBW-electrolyte by the PBWNiCu-electrolyte for PEO (Fig. 6b). In the latter case, one deals with PEO coating having its own catalytic activity instead of that of inert secondary carrier. One can see that the composites 0.2Pt/γ-Al_2O_3/Al and 0.1 Pt/NiO + CuO + γ-Al_2O_3/Al have similar values of T_{50} indicating to their comparable activity. Thus, taking into account lower concentration of noble metal in the latter case, the optimal result is obtained when catalytically active composition is deposited on substrates having their own catalytic activity.

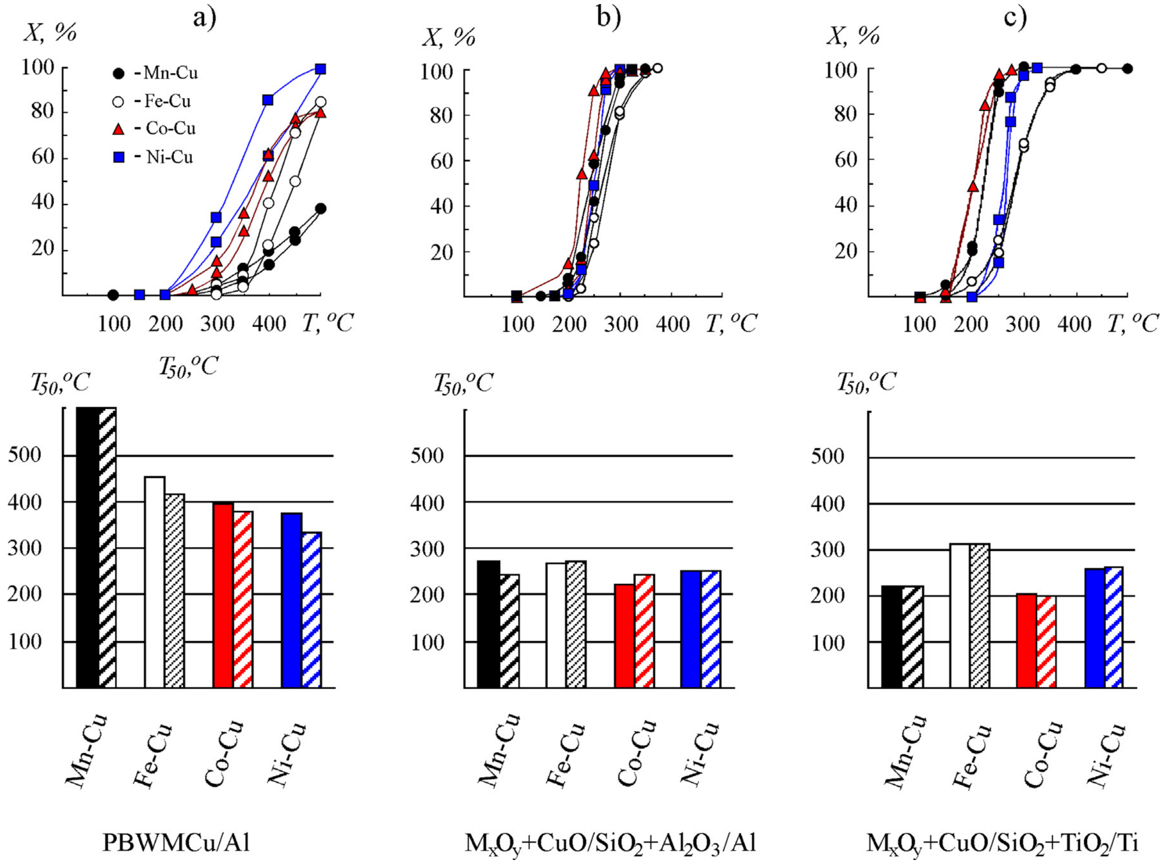

Fig. 4. Temperature dependences of CO conversion X (%) and the temperature of half-conversion T_{50} (°C) for the samples with the M + Cu- containing coatings formed by method I (a) and by method II on AMg5 aluminum alloy (b) and on VT1-0 titanium (c). The dependences X = f(T) and values of T_{50} correspond to second cycles of catalytic tests.

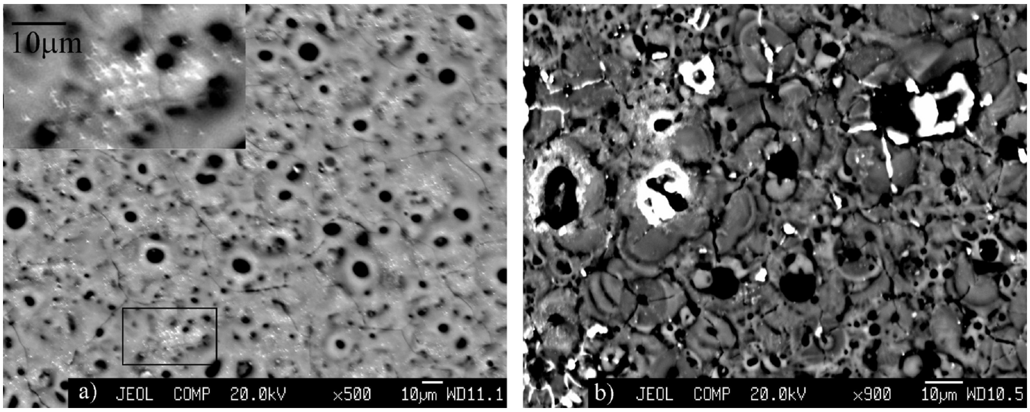

Fig. 5. SEM images of Pt-containing coatings obtained on titanium by method I in $Na_6P_6O_{18}$ + H_2PtCl_6electrolyte (a) and on aluminum alloy by method II (b) – PEO in PBW-electrolyte + single impregnation in 0.038 M solution of H_2PtCl_6. The insert at the Fig. 5a shows arrays of disperse platinum-enriched particles.

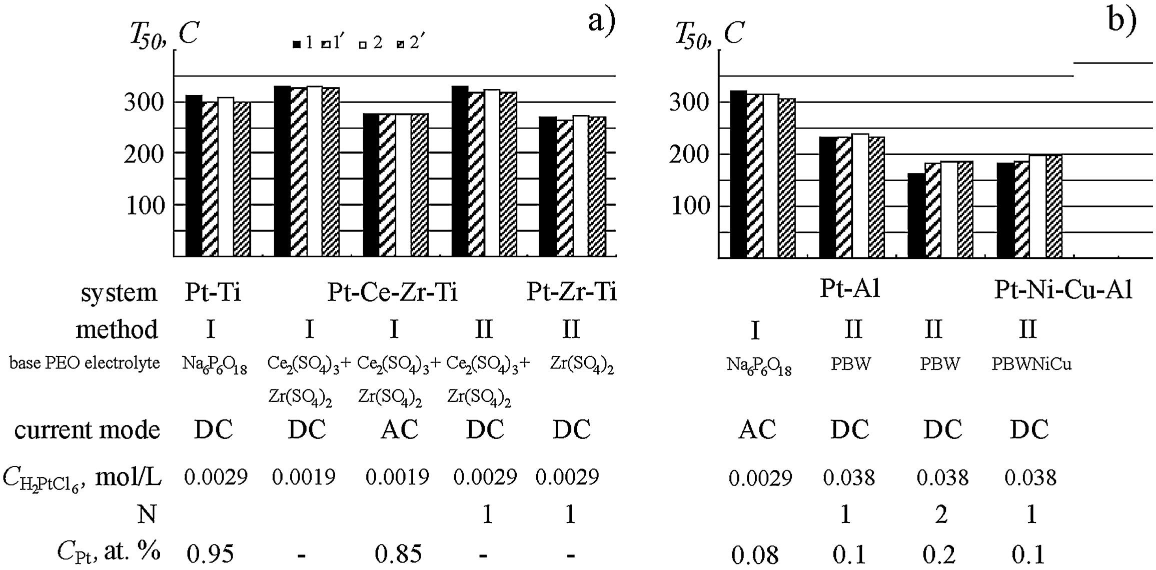

system	Pt-Ti	Pt-Ce-Zr-Ti			Pt-Zr-Ti
method	I	I	I	II	II
base PEO electrolyte	$Na_6P_6O_{18}$	$Ce_2(SO_4)_3$+ $Zr(SO_4)_2$	$Ce_2(SO_4)_3$+ $Zr(SO_4)_2$	$Ce_2(SO_4)_3$+ $Zr(SO_4)_2$	$Zr(SO_4)_2$
current mode	DC	DC	AC	DC	DC
$C_{H_2PtCl_6}$, mol/L	0.0029	0.0019	0.0019	0.0029	0.0029
N				1	1
C_{Pt}, at. %	0.95	-	0.85	-	-

	Pt-Al			Pt-Ni-Cu-Al
	I	II	II	II
	$Na_6P_6O_{18}$	PBW	PBW	PBWNiCu
	AC	DC	DC	DC
	0.0029	0.038	0.038	0.038
		1	2	1
	0.08	0.1	0.2	0.1

Fig. 6. Comparing the temperature of half-conversion CO in the first (1, 1') and second (2, 2') cycles of catalytic tests for Pt-containing coatings formed by methods I and II on titanium (a) and aluminum alloy (b). Digits (1, 2) and digits with strokes (1', 2') refer to T_{50} determined at heating and cooling of the samples, correspondingly.

3.3. Evaluation of reaction rate and activation energy in CO oxidation

Some catalytic tests were carried out on *BI-CATr-EXP* flow-circulation system to evaluate the reaction rate (for 50% conversion) W_{50} and the activation energy E_a (Fig. 7, Table 5). The composites with the highest platinum concentration (0.2Pt/γ-Al_2O_3/Al) clearly demonstrate the highest rate of CO oxidation among the composites under study. The systems containing a noble metal together with transition metals (0.1Pt/NiO + CuO + γ-Al_2O_3/Al) have the smallest activation energy. On the other hand, the composites containing transition metals without noble metals have the highest activation energy. One should note that they are more active than Pd-containing composites (0.4 at.% Pd) obtained by the combination of PEO and template sol–gel synthesis [28]. Differences in the catalytic behavior of the systems can be caused by various reaction mechanisms.

In the course of evaluating the catalytic behavior of the systems, low specific surface area of PEO coatings should be taken into account. According to the estimates made in [8], it is equal to 0.2–0.7 m^2/g. Impregnation can increase it just 5–10-fold [31].

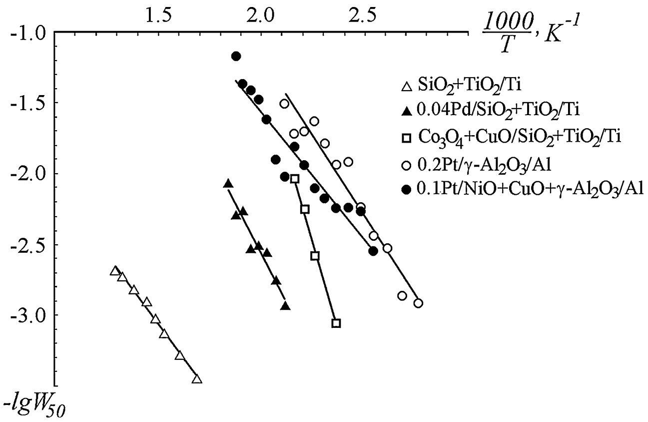

Fig. 7. Arrhenius plots $lgW_{50} = f(1000/T)$ for some composites.

Table 5
The reaction rate and the activation energy of CO oxidation for some catalysts.

Composite	Method	$W_{50} \times 10^4$ ml/g s								Evaluation of activation energy	
		100 °C	120 °C	150 °C	180 °C	200 °C	250 °C	320 °C	350 °C	Temperature range, °C	E_a, kJ/mol
$SiO_2 + TiO_2/Ti$	I							3.5	5.2	320–420	42.5
$Co_3O_4 + CuO/SiO_2 + TiO_2/Ti$	II			8.7	56.0					150–190	97.7
$0.2\ Pt/\gamma\text{-}Al_2O_3/Al$	II	13.6	36.2	116.3	196.7	310.2				90–200	43.3
$0.1\ Pt/NiO + CuO + Al_2O_3/Al$	II		28.5	56.7	114.6	95.0	427.2			120–260	34.5
$0.04Pd/SiO_2 + TiO_2/Ti$[a]	PEO + template sol–gel synthesis					11.5	54.7	106.5	104.5	200–270	54.5

[a] *Notes*: Obtaining Pd-containing coatings on titanium by combination of PEO technique and template sol–gel synthesis is reported in [28], other composites are denoted as in Table 2.

4. Conclusion

Two options of plasma electrolytic oxidation application were considered to obtain catalytically active oxide coatings containing transition (Ni, Cu, Co, Mn, Fe, W) and noble metals (Pt) on aluminum and titanium. When the precursors are directly introduced into the forming PEO electrolyte, catalytically active components are concentrated in the pores or on the coating surface as arrays of disperse particles. If the coatings are obtained by the combination of PEO technique and impregnation in precursor solutions, catalytically active components are concentrated around the pores or form a crust on the surface of the coating.

It has been found that the binary oxide cobalt–copper coatings obtained on titanium by combination of PEO and impregnation are more active in CO oxidation among the composites with transition metal oxides. Using anodic–cathodic polarization during the PEO processing of titanium in $Zr(SO_4)_2 + Ce_2(SO_4)_3 + H_2PtCl_6$ electrolyte helps to produce the coatings, which are more active in CO oxidation than similar coatings obtaining by combination of methods. Higher concentrations of H_2PtCl_6, multiplicity of impregnation, and replacement of inert-electrolyte for PEO treatment by electrolyte with precursors of transition metals are useful to ensure more active Pt-containing coatings on aluminum.

References

[1] F.C. Walsh, C.T.J. Low, R.J.K. Wood, K.T. Stevens, J. Archer, A.R. Poeton, A. Ryder, Trans. Inst. Metal Finish. 87 (3) (2009) 122.
[2] A.L. Yerokhin, X. Nie, A. Leyland, A. Matthews, S.J. Dowey, Surf. Coat. Technol. 122 (2–3) (1999) 73.
[3] I.V. Suminov, P.N. Belkin, A.V. Apelfeld, V.B. Ludin, B.L. Krit, A.M. Borisov, Plazmenno-ehlektroliticheskoe modificirovanie poverkhnosti metallov i splavov (surface plasma electrolytic modification of the metals and alloys), Moscow, 2011 (in Russian).
[4] B.L. Jiang, Y.M. Wang, Plasma electrolytic oxidation treatment of aluminium and titanium alloys, in: H. Dong (Ed.), Surface Engineering of Light Alloys, Woodhead Publishing Limited, Oxford, Cambridge/New Delhi, 2010, pp. 110–154.
[5] S.F. Tikhov, G.V. Chernykh, V.A. Sadykov, A.N. Salanov, G.M. Alikina, S.V. Tsybulya, V.F. Lysov, Catal. Today 53 (4) (1999) 639.
[6] X. Jiang, L. Zhang, S. Wybornov, T. Staedler, D. Hein, F. Wiedenmann, W. Krumm, V. Rudnev, I. Lukiyanchuk, ACS Appl. Mater. Interfaces 4 (8) (2012) 4062.
[7] N.V. Lebukhova, V.S. Rudnev, P.G. Chigrin, I.V. Lukiyanchuk, M.A. Pugachevsky, A.Yu. Ustinov, E.A. Kirichenko, T.P. Yarovaya, Surf. Coat. Technol. 231 (2013) 144.
[8] F. Patcas, W. Krysmann, Appl. Catal. A: Gen. 316 (2007) 240.
[9] F. Patcas, W. Krysmann, D. Hönicke, F.-C. Buciuman, Catal. Today 69 (2001) 379.
[10] S.A. Karpushenkov, Micro-plasma electrochemical formation of composite coatings on metals surface (Ph.D. thesis), Belarussian State Univ., Minsk, 2010 (in Russian).
[11] D.O. Misnyankin, Obtaining catalytically active oxides on aluminum from aqueous solutions by plasma-chemical method (Ph. D. thesis), Ukrainian State Univ. Chem. Technol., Dnepropetrovsk, 2006.
[12] M.V. Ved', N.D. Sakhnenko, Corrosion: Mater. Protec. 10 (2007) 36 (in Russian).
[13] RF Patent 2103057, Byull. Izobret. (2) (1998).
[14] DD Patent 248064 (1987).
[15] S. Meyer, R. Gorges, G. Kreisel, Thin Solid Films 450 (2004) 276.
[16] X.H. Wu, Z.H. Jiang, H.L. Liu, S.G. Xin, X.G. Xu, Thin Solid Films 441 (2003) 130.
[17] X.H. Wu, Q. Wei, X.B. Ding, W.D. He, Z.H. Jiang, J. Mol. Catal. A: Chem. 268 (2007) 257.
[18] Y.K. Shin, W.S. Chae, Y.W. Song, Y.M. Sung, Electrochem. Commun. 8 (2006) 465.
[19] J.F. Li, L. Wan, J.Y. Feng, Sol. Energy Mater. Sol. Cells 90 (2006) 2449.
[20] J. He, Q. Luo, Q.Z. Cai, X.W. Li, D.Q. Zhang, Mater. Chem. Phys. 129 (2011) 242.
[21] N. Salami, M.R. Bayati, F. Golestani-Fard, H.R. Zargar, Mater. Res. Bull. 47 (2012) 1080.
[22] M.R. Bayati, A.Z. Moshfegh, F. Golestani-Fard, Appl. Surf. Sci. 256 (2010) 2903.
[23] GDR Patent 273 364 (1989).
[24] N.B. Kondrikov, E.V. Shchitovskaya, M.S. Vasilyeva, V.G. Kuryavy, V.M. Bouznik, Surf. Rev. Lett. 10 (1) (2003) 101.
[25] G.I. Marinina, M.S. Vasilyeva, A.S. Lapina, A.Yu. Ustinov, V.S. Rudnev, J. Electroanal. Chem. 689 (2013) 262.
[26] D.J. Liu, B.L. Jiang, M. Zhai, Q. Li, Mater. Sci. Forum. 695 (2011) 21.
[27] N.I. Steblevskaya, M.A. Medkov, V.S. Rudnev, I.V. Lukiyanchuk, M.V. Belebeletskaya, A.V. Zorin, V.V. Permyakov, Russ. J. Appl. Chem. 86 (5) (2013) 727.
[28] I.V. Lukiyanchuk, I.V. Chernykh, V.S. Rudnev, L.M. Tyrina, E.K. Papynov, V.A. Avramenko, V.G. Kuryavy, A new approach to the synthesis of Pd-containing catalysts for CO oxidation (2013) (Part 2), in: Proceedings of 2nd Russian Conference with Invited Foreign Speakers: New Approaches to Chemical Technology of Mineral Raw Materials. Solvent Extraction and Sorption, St. Peterburg, 03–06 June, 2013, pp. 143–145.
[29] V.S. Rudnev, L.M. Tyrina, I.V. Lukiyanchuk, T.P. Yarovaya, I.V. Malyshev, A.Yu. Ustinov, Surf. Coat. Technol. 206 (2–3) (2011) 417.
[30] M.S. Vasilyeva, V.S. Rudnev, A.Yu. Ustinov, I.A. Korotenko, E.B. Modin, O.V. Voitenko, Appl. Surf. Sci. 257 (4) (2010) 1239.
[31] V.S. Rudnev, L.M. Tyrina, A.V. Zorin, V.V. Permyakov, Russ. J. Appl. Chem. 83 (9) (2010) 1576.
[32] V.S. Rudnev, S. Wybornov, I.V. Lukiyanchuk, T. Staedler, X. Jiang, A.Yu. Ustinov, M.S. Vasilyeva, Appl. Surf. Sci. 258 (22) (2012) 8667.
[33] RF Patent 1 783 004, Byull. Izobret. (47) (1992).
[34] RF Patent 2 241 541, Byull. Izobret. (5) (2005).
[35] L.M. Tyrina, V.S. Rudnev, I.V. Lukiyanchuk, A.Yu. Ustinov, V.I. Sergienko, M.S. Vasil'eva, N.B. Kondrikov, Doklady Phys. Chem. 415 (1) (2007) 183.
[36] I.V. Lukiyanchuk, V.S. Rudnev, L.M. Tyrina, P.M. Nedozorov, O.G. Berestok, Russ. J. Appl. Chem. 82 (6) (2009) 1000.
[37] I.V. Lukiyanchuk, V.S. Rudnev, I.V. Chernykh, I.V. Malyshev, L.M. Tyrina, M.V. Adigamova, Surf. Coat. Technol. 231 (2013) 433.
[38] L.M. Tyrina, V.S. Rudnev, A.Yu. Ustinov, I.V. Lukiyanchuk, P.M. Nedozorov, Inorg. Mater. 45 (4) (2009) 414.
[39] L.M. Tyrina, V.S. Rudnev, T.P. Yarovaya, A.Yu. Ustinov, I.V. Lukiyanchuk, V.V. Permyakov, Russ. J. Appl. Chem. 83 (4) (2010), 680.
[40] L.M. Tyrina, V.S. Rudnev, P.M. Nedozorov, A.Yu. Ustiniov, I.V. Lukiyanchuk, T.A. Kaidalova, Russ. J. Inorg. Chem. 56 (9) (2011) 1429.
[41] I.V. Lukiyanchuk, V.S. Rudnev, P.M. Nedozorov, Russ. J. Phys. Chem. A 84 (6) (2010) 1059.
[42] V.S. Rudnev, I.V. Lukiyanchuk, V.G. Kuryavyi, Prot. Met. Phys. Chem. Surf. 45 (1) (2009) 71.
[43] V.S. Rudnev, Surf. Coat. Technol. 235 (2013) 134.
[44] G.K. Boreskov, Kinetika i kataliz 8 (5) (1967) 1020 (in Russian).
[45] G.K. Boreskov, V.I. Marshneva, Doklady Akad. Nauk SSSR 213 (1) (1973) 112 (in Russian).
[46] Ye.V. Khokhryakov, P.I. Butyagin, A.I. Mamaev, J. Mater. Sci. 40 (2005) 3007.